*International Journal of Emerging Research in Management &Technology*
*ISSN: 2278-9359 (Volume-4, Issue-12)*

**Research Article** | **December 2015**

# The Preparation of Zinc Oxide Thin Films and the Study of Their Electrical and Optical Properties

**B. B. Dhale[1], S. H. Mujawar[2], P. S. Patil[3]**

[1]Gogate Jogalekar College, Ratnagiri. (M.S), India

[2]Mahatma Phule Mahavidhylaya, Pimpri, Pune (M.S), India

[3]Thin Film Materials Laboratory, Department of Physics, Shivaji University, Kolhapur, (M.S.) India

***Abstract:***

***Zinc oxide thin films were prepared by spray pyrolysis technique on to glass substrates and F:$SnO_2$ coated glass substrate. Zinc acetate as a precursor solution for the spray. The deposition temperature and solution concentration were varied to obtain good quality and uniform deposits. The films deposited at 350 to 500ºC deposition temperature and 0.1 to 0.4 M solution concentration. The structural and morphological properties of zinc oxide thin films were studied. Zinc Oxide thin films exhibited a direct-gap and unipolar n-type semiconductor with a band-gap of 3.25 eV. The electrical resistivity decreases with both deposition temperature and solution concentration.***

***Keywords: Zinc oxide; Optical properties; spray pyrolysis; Thin films***

## I. INTRODUCTION

ZnO is one of the promising materials in the field of nanotechnology which possesses unique optical and electrical properties. It is a unique material that exhibits semiconducting, piezoelectric, and pyroelectric multifunctional properties. ZnO has three key advantages: It is a semiconductor, has direct wide band gap energy (3.3 eV) and a large excitation binding energy (60 meV) [1]. It is an important functional oxide, exhibiting near ultraviolet emission and transparent conductivity. Secondly, ZnO is piezoelectric, which is a key property in building electromechanical-coupled sensors and transducers. Finally ZnO is a bio-safe and biocompatible. ZnO could be one of the most important nanomaterials in future application. Nanosized ZnO is a promising candidate for ultraviolet (UV) lasers, electro-optical switch, liquid crystal display (LCD) and optoelectronic devices, and consequently has attracted increasing attention in recent years [2]. It is a member of wurtzite family of structures. Nanowire based nanodevice of ZnO can realize ultraviolet lasing action at room temperature with low lasing threshold. ZnO exhibits various morphologies by varying preparative parameters. 1D nanostructures of ZnO, including nanowires, nanobelts and nanotubes have been attracting vast interest in the field of nanotechnology.

ZnO films have been prepared by several techniques such as molecular beam epitaxy [3], RF magnetron sputtering [4], chemical vapor deposition [5], spay pyrolysis [6], chemical bath deposition [7] and electrodeposition [8]. However, electrodeposition technique presents several advantages as: cost effective, possibility of large-scale deposition, low temperature processing and control over film thickness. Several studies have been devoted to the electrodeposition of oxide thin films from oxygen dissolved precursor, as for instance for cathodic deposition using nitride ions as the oxygen precursor. It has been discovered that good quality zinc oxide thin films can be deposited by using dissolved oxygen as the precursor according to overall reaction.

$$Zn^{+2} + 0.5O_2 + 2e^- \rightarrow ZnO \quad \text{---------- (1)}$$

ZnO is one of the potential semiconductor materials in dye sensitized solar cells (DSSC) due to its stability against photo corrosion and photochemical properties. ZnO exhibits good photoelectrochemical properties as compared to other wide band gap materials such as GaN [9]. The special interest is the preparation of highly nanoporous, high surface area ZnO films due to their importance in the fields of high efficiency dye-sensitized solar cells, gas sensors. The use of organic surfactants (additives) in electrodeposition solution is extremely important due to their influence on morphological and structural properties of deposits. Organic surfactants are commonly used in zinc electrodeposition to control the crystal shape and size, in order to produce smooth and bright deposits. The role of the organic surfactants is to change the morphology of the deposit owing to their concentration dependent specific activity during deposition. The array of nanotubes and ZnO microcavities were fabricated with the templates of polystyrene particles and alumina oxide by electrodeposition [10,11].

## II. EXPERIMENTAL DETAILS

Zinc oxide thin films have be deposited on to glass substrates and FTO coated conducting glass substrates using spray pyrolysis technique from zinc acetate (THOMAS BAKER, 99.5 % pure) as a precursor solution for the spray. The deposition temperature and solution concentration were varied to obtain good quality and uniform deposits. The films deposited at 350 to 500ºC deposition temperature and 0.1 to 0.4 M solution concentration are denoted by $T_1$, $T_2$, $T_3$, $T_4$, and $C_1$, $C_2$, $C_3$, $C_4$, respectively. Films deposited on the glass substrate were used for structural and morphological characterization.

 

To prepare the starting solution for the deposition of zinc oxide thin films, initially, powder of zinc acetate was used to dissolved in double distilled water. The resulting solution was then further pulverized pneumatically by means of a specially designed glass nozzle on to the preheated glass substrates. The sprayed droplets undergo evaporation, solute condensation and thermal decomposition, thereby resulting in the formation of zinc oxide thin film. During the synthesis, various preparative parameters like solution concentration, solution spray rate, nozzle to substrate distance, carrier gas flow rate etc. were optimized to obtain transparent, uniform, adhesive and pin hole free deposits.

The structural and morphological characterizations were carried out using Philips PW 3710 X-ray diffractometer with CuKα radiation (wavelength 1.5405 Å) and scanning electron microscopy (SEM) JEOL JSM 6360 respectively. The optical characterization was carried out using UV-VIS Systronic spectrophotometer in the wavelength range 350 to 850 nm. The AC conductivity of the zinc oxide films was measured using LCR meter model 4285 A Precision LCR meter. For the electrical resistivity and TEP measurements home made two point probe resistivity and TEP unit was used.

## III. RESULTS AND DISCUSSION

### 3.1. Thermo-gravimetric analysis and differential thermal analysis

The thermogram recorded for zinc acetate (THOMAS BAKER, 99.5 % pure) powder is shown in Figure 1. The thermal evolution in oxygen atmosphere takes place in four consecutive stages with weight losses for which the inflection point coincides with the temperature corresponding to the endotherms and exotherms in DTA trace. The weight loss of precursor zinc acetate ($Zn(CH_3COO)_2\ 2H_2O$) begins at 30ºC . Initially, minor weight loss in the temperature range 30–95 ºC was observed. Step I is due to the evaporation of physisorbed water from the precursor. This is followed by a slow decay of TGA curve in the temperature range of 95–200 ºC (Step-II), appeared as a rapid decay in the TGA curve during 200– 275ºC (step III) These consequent weight losses are attributed to the decay leading to the decomposition of acetate groups. A further slow weight loss at the temperature of 275 ºC, coincides with an exothermic peak, indicating the formation of ZnO phase, and becomes stable after the temperature of 350ºC (step IV). After 350ºC the DTA trace is stable with no further weight loss indicating the formation of stoichiometric ZnO phase. Thus, the TGA/DTA results indicate the formation of stoichiometric ZnO by decomposition of zinc acetate after 350º C.

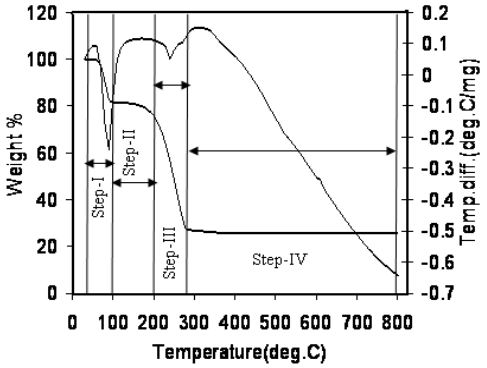


Figure1. Thermo-gravimetric analysis (TGA) and differential thermal analysis (DTA) of zinc acetate powder.

### 3.2. Structural characterstization

The structural changes and identification of phases were studied with the help of XRD technique. The diffracting angle 2θ, was varied between 10 and 100º. The XRD patterns were recorded for all the samples are shown in Figure 3.2.(a, b). The observed XRD patterns were compared with standard JCPDS data file (number 75– 1533).

The thin films deposited at various deposition temperature and solution concentrations are used for their structural characterization. The observed d-values are in good agreement with the slandered d-values. All the XRD patterns shows reflections along (002) plane at $2\theta = 34.4^o$. The peak intensity along (002) plane increases with increase in deposition temperature (Figure 3.2.a) Figure 3.2.b shows the XRD patterns for the films deposited at different solution concentrations. All the films shows preferred orientation along (002) direction at $2\theta=34.4^o$. The peak intensity of the (002) plane for all the samples increases with increase in solution concentration and deposition temperature. From the X-ray analysis pure ZnO film formation was confirmed.

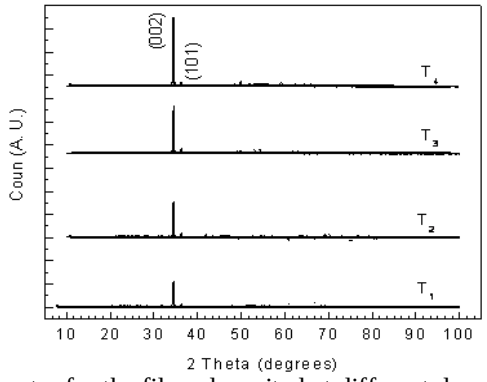


Figure 3.2.a XRD spectra for the films deposited at different deposition temperatures.

 

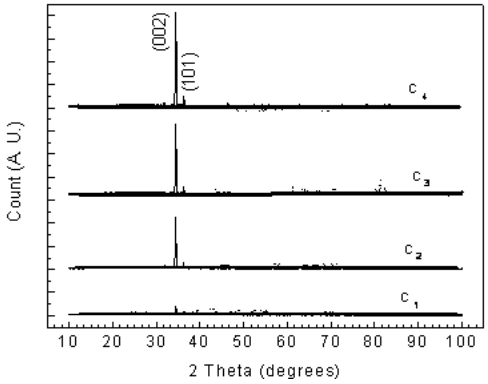


Figure 3.2.b XRD spectra for the films deposited at different solution concentrations.

**3.3. Optical absorption studies**

The optical energy band gap of ZnO thin film was estimated from optical absorption measurement. The optical absorption spectrum for the ZnO thin film is recorded in the wavelength range of 350-850 nm at room temperature. The optical absorption data were analyzed using the following classical relation (2) of optical absorption in semiconductor near band edge [15].

$$\alpha = \frac{\alpha_0 (h\upsilon - Eg)^n}{h\upsilon} \quad \text{---------- (2)}$$

where, Eg is the separation between bottom of the conduction band and top of the valence band, hν is the photon energy and n is a constant. Value of n depends on the probability of transition; it takes values as 1/2, 3/2, 2 and 3 for direct allowed, direct forbidden, indirect allowed and indirect forbidden transition respectively. Thus if plot of $(\alpha h\nu)^2$ Versus (hν) is linear the transition is direct allowed. Extrapolation, of the straight-line portion to zero absorption coefficient (α=0), leads to estimation of band gap energy (Eg) values. Figure 3.4(a, b) shows variation of $(\alpha h\nu)^2$ as a function of photon energy (hν). Figure shows that the optical band gap energy is found to be 3.25 eV for the all the films deposited at different deposition temperatures and at various solution concentrations. Tease band gap energies are in agreement with the documented room temperature values of 3.2 to 3.4 eV [16].

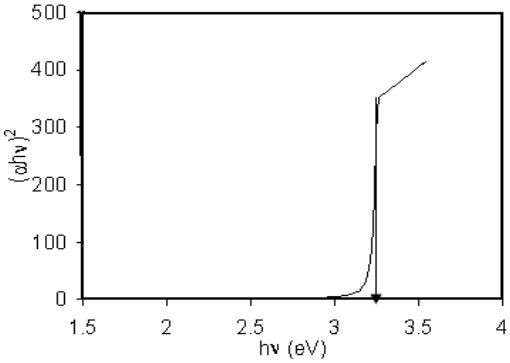


Figure 3.3.a The variation of $(\alpha h\upsilon)^2$ vs. hυ for film deposited at 450 ºC.

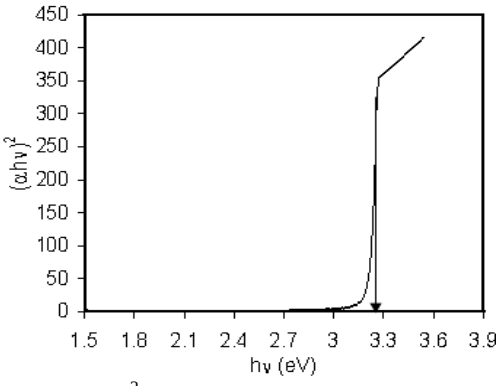


Figure 3.3.b The variation of $(\alpha h\upsilon)^2$ vs. hυ for film deposited 0.4 M solution concentration.

**3.4. Surface morphology and compositional analysis**

Figure 3.5(a,b) shows scanning electron micrographs for the films deposited at 450ºC and solution 0.4 M solution concentrations respectively. The irregular shaped grains of about 150nm size were observed for the films deposited at 450ºC (Figure 3.4.a). Relatively dense structure is observed for the films deposited at higher solution concentration (figure 3.4.b).

 

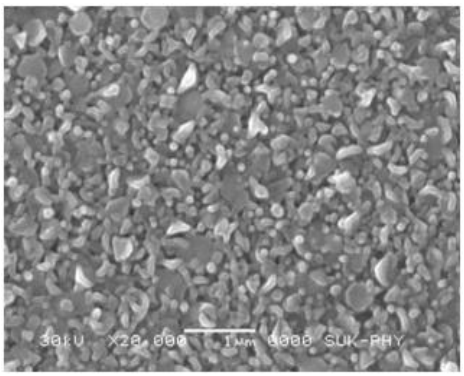

Figure 3.4.a SEM image for the film deposited at 500°C

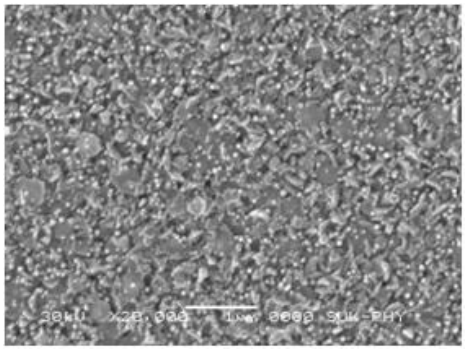

Figure 3.4.b SEM image for the film deposited 0.4 M solution concentration.

**3.5. Electrical Measurement (A.C.)**

Figure 3.6 The capacitance-voltage (C-V) measurements for the thin films deposited at various temperatures i.e. at 350°C,400°C,450°C & 500°C and also at various solution concentrations such as 0.1M, 0.2M, 0.3M, & 0.4M of ZnO were carried out using a "4285 A Precision LCR meter". The contact material on the top of the ZnO films was Silver paste, while the bottom contact layer was TCO; as shown in figure below.

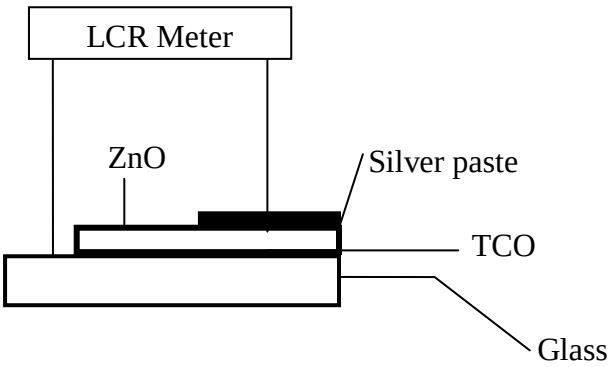


Figure 3.5 A Schematic diagram for A.C. measurements of ZnO thin films.

From the value of C-V data as shown in figure 3.6(a b.) under a fixed field of 250 KHz, it was found that the capacitance of the TCO/ZnO/Ag device increased exponentially with voltage, which is the characteristics of a Schottky junction. Similar reports were reported by A. Mondal et al. [17]

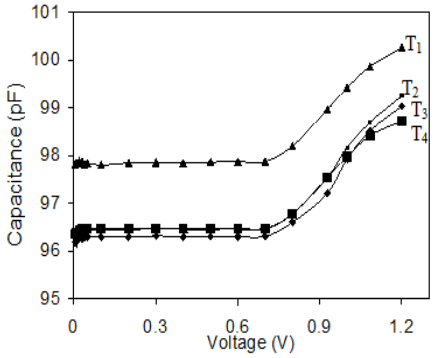


Figure 3.5.a AC conductivity measurement for the films deposited at different temperatures.

 

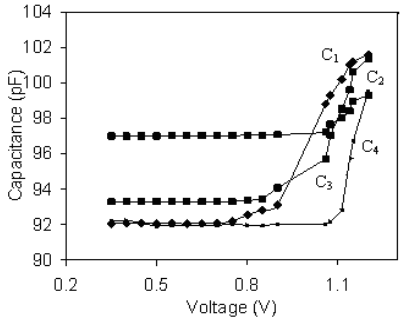


**Figure**5.8b AC conductivity measurements for the films leposited at different concentrations.

### 3.6. Electrical resistivity

The dc electrical resistivity of all the samples was measured in the temperature range of 300–650 K, using a two-point probe method. The room temperature electrical resistivity for film was of the order of $10^{-4}$ V cm. The room temperature electrical resistivity decreases with increase in solution concentration. Also it is noted that the electrical resistivity decreases with increase in temperature indicating that the samples are semiconducting. Figure 3.7.(a b) shows temperature dependence of resistivity (r) for all the samples.

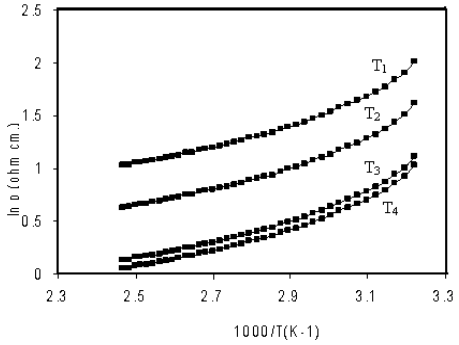


Figure3.6.a The variation of log ρ vs. (1000/T) for the films deposited at different deposition temperatures.

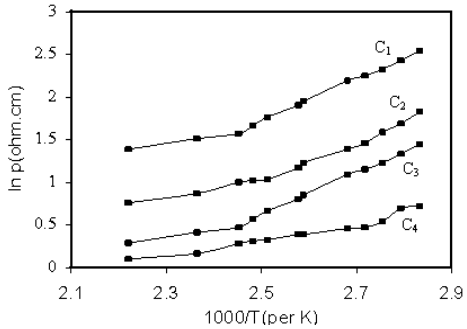


Figure 3.6.b The variation of log ρ vs. (1000/T) for the films deposited at different solution concentrations.

### 3.7. Thermoelectric power measurement

Thermoelectric power is the ratio of thermally generated voltage to the temperature difference in the semiconductor. This gives the information about charge carriers in the given material. The thermo-emf of all the films was measured as a function of temperature in the range of 300–450 K using the TEP unit. From the polarity of thermally generated voltage at hot end, it is concluded that the films exhibit an n type electrical conductivity. The variation of thermo-emf with temperature difference (ΔT) for all the samples is shown in Figure 3.8(a,b). The thermo-emf increases with increase in temperature difference. The TEP decreases with increase solution conc.

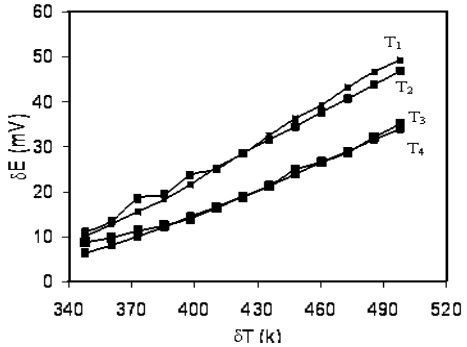


Figure 3.7.a The variation of thermo-emf Vs temp.diff.ΔT for films deposited at different deposition temperature.

 

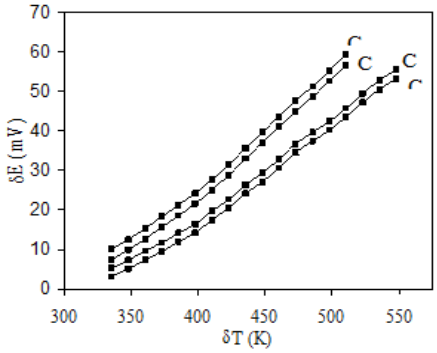


Figure 3.7.b The variation of thermo-emf Vs temp.diff.ΔT for films deposited at different solution concentrations.

## IV. CONCLUSIONS

*n*-ZnO thin films have been successfully deposited using pneumatic spray pyrolysis technique. From the X- ray analysis pure ZnO formation and textured film formation along (002) plane was confirmed. The structural characterization was supported by band gap energy determination and is found 3.25 eV. SEM images for the films deposited at higher deposition temperature shows well defined grains than the films deposited at higher solution concentrations. The electrical resistivity decreases with both deposition temperature and solution concentration. From the thermo-emf measurements the n-type conductivity was confirmed.

## REFERENCES

[1] Z. L. Wang, J. Phys. Condense Matter, 303 (2004) R829.
[2] A. I. Inamdar, S. H. Mujawar, S. B. Sadale, A. C. sonavane, M. B. Shelar, P. S. Shinde, P. S. Patil, Sol. Energy Matar. So. Cells, 91 (2007) 864.B.
[3] Y. Chen, D.M. Bagnall, H. J. Koh, K.T. Park, K. Hiraga, Z. Zhu, T. Yao, J. Appl. Phys. 84 (1998) 3912.
[4] M.A. Martinez, J. Herrero, M.T. Gutierrez, Sol. Energy Mater. Sol. Cells 45 (1997) 75.
[5] H. Sato, T. Minami, T. Miyata, S. Takata, M. Ishii, Thin Solid Films 246 (1994) 65.
[6] M.G. Ambia, M.N. Islam, M.O. Hakim, J. Mater. Sci. 29 (1994) 6575.
[7] A. Ennaoui, M. Weber, R. Scheer, H.J. Lewerenz, Sol. Energy Mater. Sol. Cells 54 (1998) 277.
[8] M. Izaki, T. Omi, Appl. Phys. Lett. 68 (1996) 2439.
[9] F. K. Shan, B. C. Shin, S. C. Kim, Y. S. Yu J. Korean Phys. Soc. 42 (2003) S1174.
[10] L. Yanbo, Z. Maojun, L. Ma, M. Zhong, W. Shen. Inorg. Chem. 47 (2008) 3140.
[11] Y. Gao, M. Nagai, Longmuir, 22 (2006) 3936.
[12] H. Yoshikawa, S. Adachi, Jpn. J. Appl. Phys. 36, No. 10 (1997) 6237.
[13] M. D. Archer, J. Appl. Elec. 5 (1975) 17.
[14] X. Gan, Gao, J. Qiu, Li, Appl. Sur. Sci. 254 (2008) 3839.
[15] R.K. Kawar, P.S. Chigare, P.S. Patil, Appl. Surf. Sci. 206 (2003) 90.
[16] E. A. Dalchiele, P. Giorgi, R. E. Morotti, F. Martin, J. R. Ramos-Barrado, R. Ayouci, D. Leinen, Solar Energy Materials & Solar Cells, 70 (2001)245.
[17] A. Mondal, N. Mukherjee, S. Kumar Bhar, Materials Letter 60 (2006)748.

 